

# **Conjugation, labelling and *in vitro/in vivo* assessment of an anti-VEGF monoclonal antibody labelled with niobium isotopes.**

A.de la Fuente<sup>1</sup>, V. Radchenko<sup>1</sup>, T.Tsotakos<sup>2</sup>, C. Tsoukalas<sup>2</sup>, M. Paravatou-Petsotas<sup>2</sup>, A. L. Harris<sup>3</sup>, U.Koester<sup>4</sup>, F. Roesch<sup>\*1</sup>, P. Bouziotis<sup>2</sup>

<sup>1</sup>Institute of Nuclear Chemistry, Johannes Gutenberg University, Mainz, Germany

<sup>2</sup>Institute of Nuclear & Radiological Sciences & Technology, Energy & Safety, N.C.S.R. “Demokritos”, Athens, Greece

<sup>3</sup>Weatherall Institute of Molecular Medicine, University of Oxford, Oxford, U.K.

<sup>4</sup> Institute Laue-Langevin Neutron Science and Technology, Grenoble, France.

\* Author for correspondence

Prof. Dr. Frank Roesch, Institut für Kernchemie, Johannes Gutenberg Universität Mainz, Fritz-Strassmann-Weg 2  
D-55128 Mainz, Germany

E-mail: [frank.roesch@uni-mainz.de](mailto:frank.roesch@uni-mainz.de)

**Keywords:** <sup>90/95</sup>Nb / Bevacizumab / labelling / VEGF / biodistribution/ *immuno*-PET

## ABSTRACT

$^{90}\text{Nb}$  is a positron emitting radionuclide that exhibits attractive characteristics for use in the design and synthesis of radioimmunoconjugates. In the current study we investigate  $^{90}\text{Nb}$  as a possible future isotope for *immuno*-PET. Prior to  $^{90}\text{Nb}$  *in vivo* studies, this paper describes *in vitro* and *ex vivo* studies using a  $^{95}\text{Nb}$ -monoclonal antibody analogue.  $^{95}\text{Nb}$  has a half-life of 35 days and is convenient for long-term studies.  $^{95}\text{Nb}$ -labelled bevacizumab was evaluated for early antiangiogenic tumor response assessment and the results were compared with other well established PET nuclides for *immuno*-PET.

### Methods:

Bevacizumab was modified with Df-Bz-NCS (Df) and labelled with  $^{95}\text{Nb}$  which was previously separated from irradiated natural Zr in a multistep procedure. Stability of  $^{95}\text{Nb}$ -Df-Bevacizumab was evaluated in saline and in human plasma over 7 days. Biodistribution *ex vivo* studies were performed in tumor-bearing mice.

### Results:

$^{95}\text{Nb}$  was obtained in high purity and high specific activity in 200  $\mu\text{L}$  oxalic acid 0.1 M, ready for labelling. We show a successful labelling strategy and a high *in vitro* stability of  $^{95}\text{Nb}$ -Df-bevacizumab, *ex vivo* studies displayed good tumor-to-background ratios, optimum after 2 d p.i., when 20  $\mu\text{g}$  of antibody per mouse were injected.

### Conclusions:

$^{95}\text{Nb}$  was successfully produced and purified from the irradiated target. Labelling of pre-modified bevacizumab with desferrioxamine was achieved in high yields. *In vitro* stability of  $^{95}\text{Nb}$ -Df-bevacizumab has been demonstrated, and *ex vivo* biodistribution studies showed specific tumor uptake in M165 tumor-bearing mice. *In vivo* studies with  $^{90}\text{Nb}$ -Df-bevacizumab and small animal PET are in preparation.

## 1 INTRODUCTION

The application of radionuclide-labelled biomolecules such as monoclonal antibodies or antibody fragments for imaging purposes is called *immunoscintigraphy*. More specifically, when the nuclides used are positron emitters, the technique is referred to as *immuno-PET* which combines the high sensitivity and resolution of a PET camera with the specificity of a monoclonal antibody (mab).

In personalized therapeutic strategy, *immuno-PET* provides the confirmation of both tumor expression and verification of the mab accumulation, thus being a key tool in treatment evaluation (Van Dongen et al., 2007).

Currently, there is an urgent need for radionuclides with a half-life which correlates with the biological kinetics of biomolecules under question. Radionuclide candidates have to match some features to be used for *immuno-PET*. The most important ones are: i) a half-life paralleling the biological half-life of the mAb; ii) a high positron branching with no or weak accompanying radiation ( $\beta^-$ ,  $\gamma$ ); iii) a preferably low  $\beta^+$ -energy to allow high-resolution PET imaging; iv) the availability of the radionuclide, i. e. an efficient production and radiochemical separation route and v) a facile, efficient and stable coupling to mAbs as well as maintenance of the *in vivo* biological characteristics of the antibody. Nowadays the following positron emitters are under investigation for *immuno-PET*:  $^{76}\text{Br}$  ( $t_{1/2}$  16.2 h) (Tolmachev, 2011),  $^{86}\text{Y}$  ( $t_{1/2}$  14.7h) (Nayak and Brechbiel, 2011)  $^{64}\text{Cu}$  ( $t_{1/2}$  14 h) (Chang et al., 2013),  $^{89}\text{Zr}$  ( $t_{1/2}$  78.4h) (Vugts et al., 2013; Verel et al., 2003; Severin et al., 2011) and  $^{124}\text{I}$  ( $t_{1/2}$  100.3h) (Chacko et al., 2014) Table 1.

**Here table 1**

Due to the slow pharmacokinetics of intact antibodies, positron-emitting radionuclides with long and medium-long half-lives are of interest for PET-imaging with antibodies, therefore  $^{68}\text{Ga}$  and  $^{18}\text{F}$ , which are common nuclides in routine PET imaging applications, are not suitable.  $^{90}\text{Nb}$  is a promising candidate due its half-life of 14.6 hours and low  $\beta^+$  energy of  $E_{\text{mean}} = 0.35 \text{ MeV}$  (Tolmachev, 2011).

In previous reports we have proposed  $^{90}\text{Nb}$  as a promising candidate for application in *immuno*-PET (Radchenko et al., 2012; Radchenko et al., 2016; Busse et al., 2002 a,b) since its half-life of 14.6 hours and a high positron branching of 53% may make  $^{90}\text{Nb}$  an ideal candidate for application with monoclonal antibodies and antibody fragments.

The humanized monoclonal antibody bevacizumab was the antibody chosen for the experiments as currently many studies are concentrating on the labeling of bevacizumab with radionuclides for its *in vivo* behaviour evaluation (Chang et al., 2013; Radchenko et al., 2016, Nagengast et al., 2007; Nagengast et al., 2010; Nayak et al., 2011; Stollman et al., 2008). Bevacizumab plays a key role in angiogenesis, as it binds all vascular endothelial growth factor-A (VEGF-A) isoforms, preventing them from binding to receptors, thus blocking the biologic pathways induced after VEGF binding (Ferrara et al., 2005). By blocking the receptors, the growth of vascular endothelial cells derived from arteries and veins, which are necessary to supply solid tumors with oxygen and nutrients, is highly diminished.

The search for sensitive technologies to monitor anti-angiogenic response *in vivo* is an ongoing one. It has previously been shown that radiolabeled bevacizumab can be used for *in vivo* VEGF visualization and quantification, due to its interaction with the larger isoforms of VEGF-A that are associated with the surface and/or the extracellular matrix (Stollman et al., 2009). Our research efforts are focused on the development of  $^{90}\text{Nb}$ -bevacizumab as an alternative PET imaging agent for *in vivo* monitoring of VEGF-A levels.

In order to introduce  $^{90}\text{Nb}$  as a novel positron emitter for *immuno*-PET, we have assessed the *in vitro* stability of  $^{95}\text{Nb}$  radiolabeled bevacizumab, as well as its cell binding capacity to breast cancer cells transfected with the VEGF-165 isoform. Furthermore, biodistribution studies on tumor-bearing SCID mice were performed, in order to demonstrate the *in vivo* behavior of the radiolabeled antibody.

## 2 MATERIALS AND METHODS

### 2.1 Materials

Reagents were purchased from Sigma-Aldrich (Germany) and used without further purification, unless otherwise stated. Deionized water ( $18\text{ M}\Omega\text{ cm}^{-1}$ ) and ultra pure HCl solution were used. No further special measures were taken regarding working under strict metal-free conditions. Bevacizumab (Avastin<sup>®</sup>, Roche) was bought from Roche Ellas S. A. (Greece). For the purification of conjugated and labeled antibodies, PD-10 columns (GE Healthcare Life Science) were applied, for ion exchange separation Aminex A27,  $15 \pm 2\text{ }\mu\text{m}$  and AG1x8, 200-400 mesh anionic exchange resins and DOWEX 50x8, 200-400 mesh (BioRad) were used. For solid extraction, UTEVA<sup>®</sup> resin (Triskem Int., France) was applied.

The production yield, radionuclidic purity, radiochemical purity and separation yield of  $^{95}\text{Nb}$  were determined by  $\gamma$ -ray spectroscopy using an Ortec HPGe detector system and Canberra Genie 2000 software. The dead time of the detector was always kept below 10%. The detector was calibrated for efficiency at all positions with the certified standard solution QCY48, R6/50/38 (Amersham, UK).

VEGF165-transfected MDA MB 213 cells (M165) were cultured at safety level I in minimum essential medium (Eagle) with 2 mM L-glutamine in the presence of 10% fetal bovine serum, at 37 °C in a humidified 5% CO<sub>2</sub> incubator.

Labeling efficiency and stability of <sup>90</sup>Nb-Df-bevacizumab was monitored by instant thin layer chromatography (iTLC) and high performance liquid chromatography (HPLC). iTLC was performed on chromatography strips (Biodex, NY). As mobile phase, 0.02 M citrate buffer (pH 5.0) was used. HPLC monitoring was performed on a Waters HPLC system using a TSKgel G3000SWXL size exclusion column (TOSOH Bioscience, Germany). As eluent, a mixture of 0.05 M sodium phosphate and 0.15 M sodium chloride (pH 6.8) solution was used at a flow rate of 0.8 mL/min.

Statistical analysis was performed using the t-test. A *p* value less than 0.05 was considered statistically significant.

## **2.2 Production of <sup>95</sup>Nb**

<sup>95</sup>Nb (*t*<sub>1/2</sub> = 35 d) was employed for biodistribution experiments to cover longer periods of time. It was produced via the <sup>94</sup>Zr (n, γ) → <sup>95</sup>Zr (β<sup>-</sup>, *t*<sub>1/2</sub> = 64 d) → <sup>95</sup>Nb reaction from natural zirconium foil (Alfa Aesar, USA). Neutron irradiation was performed at the reactor at Institute Laue-Langevin in Grenoble, France.

The production of the radionuclides <sup>95</sup>Zr / <sup>95</sup>Nb was monitored by gamma ray spectroscopy, via emissions at 724.2 keV (44.2%) and 756.7 keV (54.0%) for <sup>95</sup>Zr, and at 765.8 keV (100%) for <sup>95</sup>Nb.

## **2.3 Separation and purification of n.c.a. <sup>95</sup>Nb**

Initial attempts to separate and purify n.c.a.  $^{95}\text{Nb}$  provided samples of relatively low radioactive concentration. An alternative separation/purification strategy, leading to higher radioactive concentration of  $^{95}\text{Nb}$ , has been described elsewhere (Radchenko et al., 2012). Briefly, the irradiated zirconium target, dissolved in 21 M HF, was passed through a cation exchange resin (DOWEX 50x8, 100 mg, 200-400 mesh, 10x5 mm) resin in  $\text{F}^-$  form for the removal of colloids, unsolved target particles and possible trace contamination of  $2^+$  and  $3^+$  charged metal cations, such as for example  $\text{Cu}^{2+}$  or  $\text{Fe}^{3+}$  from the target holder. The column was additionally washed with concentrated hydrofluoric acid (1 mL). This solution (3 mL) was transferred to an anion exchange column (300 mg, 25x5 mm) filled with AG 1x8 resin (200-400 mesh) in the  $\text{F}^-$  form.  $^{95}\text{Nb}^{\text{V}}$  remained on this resin and the bulk amount of  $\text{Zr}^{\text{IV}}$  passed through. The column was washed with concentrated HF (4.5 mL) to elute traces of  $\text{Zr}^{\text{IV}}$ , while  $^{95}\text{Nb}$  stays on the column. A small plastic column was filled with UTEVA resin (150  $\mu\text{m}$ , 300 mg, 25 x 5 mm). The aforementioned anion exchange column was directly connected with the UTEVA column and 4 mL of 0.3 M oxalic acid/ 7.7 M HCl were passed through both columns. The UTEVA column was next washed with 5 M HCl (5 mL). Traces of  $\text{Zr}^{\text{IV}}$  passed through the UTEVA, while  $^{95}\text{Nb}^{\text{V}}$  remains absorbed on the column. For elution of  $^{95}\text{Nb}$  0.1 M oxalic acid was applied. The column was washed with 200  $\mu\text{L}$  and  $^{95}\text{Nb}$  eluted with another 400  $\mu\text{L}$  of 0.1 M oxalic acid.

## **2.4 Monoclonal antibody modification with Df-Bz-NCS**

Desferrioxamine has been shown to be an appropriate chelate for Nb (Radchenko et al., 2014). Bevacizumab was pre-modified with the bifunctional chelator Df-Bz-NCS following the protocol for  $^{89}\text{Zr}$  labelling from (Vosjan et al., 2010). In short, a threefold molar excess of Df-Bz-NCS (in 20  $\mu\text{L}$  DMSO) was added to 5 mg of the mab in 1 ml 0.1 M  $\text{NaHCO}_3$  buffer, pH 9.0, and

incubated for 30 min at 37 °C. Non-conjugated chelator was separated by size exclusion chromatography (SEC) using a PD-10 column and saline as the eluent.

## **2.5 Labelling of bevacizumab with $^{95}\text{Nb}$**

A purified  $^{95}\text{Nb}$  fraction in 0.1 M oxalic acid (20-100  $\mu\text{L}$ ) was mixed with 300  $\mu\text{L}$  of 0.9% sodium chloride solution and then the mixture was adjusted to pH 6-7 with 0.1 M  $\text{Na}_2\text{CO}_3$  (50-60  $\mu\text{L}$ ). The modified mab (150-300  $\mu\text{g}$ , 120  $\mu\text{L}$ ) was then added to this mixture and the volume of the mixture was adjusted to 1 mL with normal saline. The mixture was incubated at room temperature for 60 min. Finally,  $^{95}\text{Nb}$ -Df-Bz-NCS-bevacizumab was purified using a PD-10 column, with 0.9% sodium chloride solution as the mobile phase. Analysis of the product was monitored by ITLC (0.02 M citric acid/ACN, 90/10) and HPLC using a TSKgel G3000SWXL size exclusion column (TOSOH Bioscience, Germany) and as eluent, a mixture of 0.05M sodium phosphate and 0.15M sodium chloride (pH 6.8) solution at a flow rate of 0.8mL/min for 60 min.

## **2.6 *In vitro* metabolic stability**

Metabolic stability of  $^{95}\text{Nb}$ -Df-bevacizumab was studied in normal saline at room temperature and in fresh human plasma at 37°C. For preparation of human plasma, human blood was collected in heparinized polypropylene tubes and centrifuged at 5000 rpm at 4°C for 5 min. The plasma was collected and three fold excess (300  $\mu\text{L}$ ) was incubated with  $^{95}\text{Nb}$ -Df-bevacizumab (100  $\mu\text{L}$ ) at 37°C. Aliquots of the sample were withdrawn, treated with ethanol (2:1 EtOH/aliquot, v/v) and analyzed by ITLC and HPLC.

## **2.7 Immunoreactivity**



The immunoreactivity of radiolabelled bevacizumab was determined using a VEGF ELISA assay, as described by (Collingridge et al.). Briefly, 96-well ELISA plates were coated with 100 µl human VEGF165 (5 µg/ml, R&D Systems; Oxfordshire, United Kingdom) overnight in bicarbonate coating buffer (15 mM Na<sub>2</sub>CO<sub>3</sub>, 35 mM NaHCO<sub>3</sub>, pH 9.6) at 4 °C. As a next step, wells were blocked with 100 µl of 1% BSA in PBS. The wells were then washed three times with PBS and 0.1% Tween 80. Radiolabelled bevacizumab was diluted to 10 ng/ml, added to the wells (100 µl) and allowed to bind for 2 h at room temperature. After incubation, the unbound antibody was removed, the wells were washed three times with PBS and 0.1% Tween 80, and the bound antibody was solubilized with 0.2 M NaOH. The total radioactivity added to each well and the radioactivity from bound antibody was measured on a multisample γ-counter system Packard Minaxi 5500 equipped with a 3'' NaI (TI) crystal. Immunoreactivity of the antibody was calculated as *bound counts x 100/total counts*. Experiments were repeated three times.

## 2.8 Cell binding experiments

For the cell binding experiments, MDA MB 231 human breast cancer cells stably transfected with the VEGF-165 isoform were used. These M165 cells overexpressing VEGF-165 were cultured in DMEM supplemented by 10% (v/v) fetal bovine serum (FBS) 100 U/mL penicillin and 100 µg/mL streptomycin. Cells were kept in a controlled humidified atmosphere containing 5% CO<sub>2</sub> at 37° C.

On the previous day of the experiment, cells were seeded in 24-well plates and grown to confluency. For the binding experiment, increasing concentrations of the labelled antibody (0.4, 0.8, 2.0, 4.0, and 10.0 nM) were added to each well. Triplicates of each concentration were incubated at 37° C for 60 min. In order to assess specificity of binding, M165 cells in some of the wells were pretreated with an excess of unlabeled bevacizumab (125 µg). The supernatant was then removed, the cells were washed three times with ice-cold PBS, and the bound antibody was

solubilized with 0.2 M NaOH. The total radioactivity added to each well and radioactivity from bound antibodies was measured in a gamma counter.

## **2.9 Biodistribution studies**

All animal experiments were performed in compliance with EC Directive 86/609 and its implementation in national legislation (updated version EL 56/2013). Female athymic SCID mice (average weight 20 g, 5 weeks) were obtained from the breeding facilities of the Institute of Biology of the NCSR “Demokritos”. The SCID mice were inoculated subcutaneously into the right front leg with M165 cells ( $1 \times 10^7$  cells/animal) in 100  $\mu$ L fetal bovine serum-free medium. When tumors reached a size of 0.2 to 1 g (i.e. 10 to 15 days), biodistribution studies were performed.

Tumor-bearing mice were injected with 100  $\mu$ L of  $^{95}\text{Nb}$ -Df-bevacizumab [(270 kBq/20  $\mu$ g or 2.03 TBq/mmol (54.83 mCi/mmol)] via the tail vein. Groups of three animals were sacrificed at 1, 2 and 4 days post-injection.

To prove specific binding of the  $^{95}\text{Nb}$ -Df-bevacizumab to the tumor, blocking experiments were performed in the tumor-bearing mice. A group of animals was treated with 125-fold excess of the cold bevacizumab (2500  $\mu$ g /100  $\mu$ L) and after 24 hours, these animals were injected with 270 kBq/20  $\mu$ g [2.03 TBq/mmol (54.83 mCi/mmol)]  $^{95}\text{Nb}$ -Df-bevacizumab and sacrificed at 4 days after injection of the labelled antibody.

Tumors, tissues and organs (blood, heart, liver, stomach, intestines, spleen, muscle, lungs, pancreas, muscle and bones) were excised, blotted dry and weighed. Samples were counted in a gamma counter (NaI gamma counter, Packard). Standards were prepared from the injected material and were counted each time simultaneously with the tissues excised, allowing for calculations to be corrected for physical decay of the radioisotope. Radiolabelled antibody distribution over time was expressed as injected dose per gram (%ID/g).

### **3. Results**

#### **3.1 Production of $^{95}\text{Nb}$**

Niobium-95 was produced at a neutron flux of  $1.5 \times 10^{15} \text{ s}^{-1} \cdot \text{cm}^{-2}$ . A 5-day irradiation of 356.2 mg of natural Zr produced more than 1.5 GBq  $^{95}\text{Zr}$  in ILL High Flux Reactor. The maximum daughter activity of  $^{95}\text{Nb}$  generated from  $^{95}\text{Zr}$  was obtained at ~67 d EOB.

#### **3.2 Separation and purification of no-carrier added $^{95}\text{Nb}$**

The overall separation proceeds with a yield of 95-98% of  $^{95}\text{Nb}$ , collected in 400  $\mu\text{L}$  0.1 M oxalic acid with the whole separation procedure lasting less than one hour. Decontamination after UTEVA purification is  $3 \times 10^8$  which equals to 0.77 ng of zirconium present in the final fraction for a portion of 260 mg zirconium target.

#### **3.3 Preparation of $^{95}\text{Nb}$ -labeled Df-Bz-NCS- bevacizumab**

Labelling kinetics indicate a yield of  $\geq 80\%$  already at 15 min, increasing to more than 90% after 50 min. The final labelling yield with  $^{95}\text{Nb}$  was  $\geq 95\%$  (96% ITLC, 95% HPLC) after 1 hour. After SEC separation on a PD-10 column, the  $^{95}\text{Nb}$ -Df-bevacizumab had a radiochemical purity of 99%. The specific activity was 2.03 TBq/mmol (54.83 mCi/mmol)].

#### **3.4 *In vitro* stability**

After 7 days of incubation of  $^{95}\text{Nb}$ -Df-bevacizumab in NaCl 0.9% solution at 37°C and RT,  $\geq 95\%$  (99% HPLC, 97% ITLC) was still detected. Stability testing in fresh human serum at 37°C

showed a slightly higher product degradation. After 3 days of incubation  $\geq 94\%$  (97% HPLC, 94% ITLC) of labelled product was available, while at 7 days  $\geq 86\%$  (89% HPLC, 86% ITLC) of the product was still intact.

### **3.5 Immunoreactivity and cell binding experiments**

An immunoreactivity assay was performed to ascertain the biological integrity of the labeled  $^{95}\text{Nb}$ -Df-bevacizumab, the result of which is shown in Figure 1. For reasons of comparison, the immunoreactivity of  $^{99\text{m}}\text{Tc}$  labeled bevacizumab is also shown.

**Here figure 1**

*In vitro* binding studies performed on M165 cells showed a very low overall percentage of  $^{95}\text{Nb}$ -Df-bevacizumab binding, compared to the initially added activity ( $\sim 2\%$ ), and the binding of the radiolabeled antibody was diminished when the cells were pretreated with an excess of cold bevacizumab (unblocked vs blocked cells). We are thus led to the conclusion that  $^{95}\text{Nb}$ -Df-bevacizumab mainly bound to the secreted VEGF-165, but also showed selectivity for the cell-associated VEGF-165.

**Here figure 2**

### **3.6 Biodistribution**

Biodistribution of  $^{95}\text{Nb}$ -Df-bevacizumab, at an injected dose of 270kBq/20 $\mu\text{g}$  [2.03 TBq/mmol (54.83 mCi/mmol)] per mouse was performed in tumor-bearing mice (Figure 3).

**Here Figure 3**

At all time-points, the levels of radiotracer in most tissues (blood, liver, spleen, lungs, heart, stomach, intestines and pancreas) were less than those in the tumor. Tumor uptake showed a decreasing pattern in time ( $9.42 \pm 3.75$  %ID/g and  $1.21 \pm 0.38$  %ID/g at 1 and 4 days p.i., respectively), however the tumor-to-blood ratios increased from 1 to 2 days p.i. (3.58 and 5.11 respectively), showing a slight drop at 4 days p.i (4.69), cf. Table 2.

**Here Table 2**

Specificity of tumor targeting was assessed by injecting tumor-bearing mice with an excess of unlabelled bevacizumab, also shown in Figure 4. When mice were given unlabeled bevacizumab 1 day prior to  $^{95}\text{Nb}$ -Df-bevacizumab and sacrificed 4 days later, the %ID/g in the tumor decreased by ~50 %, compared with unchallenged mice ( $0.68 \pm 0.02$  %ID/g vs  $1.21 \pm 0.38$  %ID/g respectively). The %ID/g for the other tissues did not decrease, on the contrary  $^{95}\text{Nb}$ -Df-bevacizumab showed a slight increase after pretreatment with unlabeled bevacizumab.

#### **4. Discussion**

During the past decade a number of antiangiogenic agents such as sorafenib, an inhibitor of several tyrosine protein kinases, and ranibizumab, a monoclonal antibody that inhibits VEGF-A, have been US FDA approved. An important issue that needs our attention is the careful selection of patients that are most likely to respond to a specific antiangiogenic treatment. Nuclear imaging modalities have been explored as a possible way to screen patients for antiangiogenic therapy. Previous groups have demonstrated that radiolabeled bevacizumab accumulates in VEGF-A expressing tumors, and has thus been investigated as a potential SPECT and PET imaging agent for the selection of patients who are likely to benefit from antiangiogenic therapies (Nagengast et al., 2007; Nagengast et al., 2010; Nayak et al., 2011; Stollman et al., 2008). More specifically, Nagengast *et al* were the first to report on the noninvasive measurement of VEGF-A levels in the tumor, with  $^{111}\text{In}$ - and  $^{89}\text{Zr}$ -labeled bevacizumab (Nagengast et al., 2007). Nayak *et al* recently took a step further, by reporting on the radiolabeling of bevacizumab with  $^{86}\text{Y}$  for PET imaging of VEGF-A tumor angiogenesis and as a surrogate marker for  $^{90}\text{Y}$ -based radioimmunotherapy (RIT), thus introducing a true theranostic agent, with distinct advantages over bevacizumab radiolabeled with  $^{111}\text{In}$  and  $^{89}\text{Zr}$ , which have been proposed as surrogate markers for  $^{90}\text{Y}$ -based RIT (Nayak et al., 2011).

Our focus is on the development of a novel PET imaging agent, namely  $^{90}\text{Nb}$ -DF-bevacizumab, by investigating the radiolabeling and *in vitro/in vivo* characteristics of bevacizumab radiolabeled with  $^{95}\text{Nb}$ , a convenient alternative for longer-term ex vivo biodistribution studies, due to its longer half-life ( $t_{1/2} = 35$  d) and its convenient, lower-cost production (reactor-based production). Apart from its gamma emissions,  $^{95}\text{Nb}$  decays by a beta emission of 165 keV. Therefore, what we are actually proposing in this work is a theranostic, radioimmunodiagnostic/radioimmunotherapeutic pair, i.e.  $^{90}\text{Nb}$ -Df-bevacizumab for PET imaging of VEGF-A tumor angiogenesis and  $^{95}\text{Nb}$ -Df-bevacizumab for RIT.

Immunoreactivity studies showed adequate VEGF binding of  $^{95}\text{Nb}$ -Df-bevacizumab, thus proving that bevacizumab retained its immunoreactivity post-labeling. In the case of  $^{99\text{m}}\text{Tc}$ -bevacizumab, the direct method of reducing endogenous disulfide bonds resulted in lower biological activities of the labelled antibody ( $16.11 \pm 2.66$  binding efficiency), when compared to the labelling of the antibody with  $^{95}\text{Nb}$  via the desferrioxamine chelator ( $47.98 \pm 1.62$  binding efficiency). The results acquired for  $^{95}\text{Nb}$ -Df-bevacizumab were comparable to other reported immunoreactivity data for radiolabeled bevacizumab (Nagengast et al., 2007; Nagengast et al., 2010; Nayak et al., 2011). Cell binding studies on M165 cells showed that  $^{95}\text{Nb}$ -Df-bevacizumab bound to the cells, and that binding was decreased when an excess of bevacizumab was added to the cells prior to the addition of the radiotracer.

$^{95}\text{Nb}$ -Df-bevacizumab remains intact over a long period of time. A biodistribution study was performed in tumor-bearing mice injected at 1, 2 and 4 days p.i. [ $270 \text{ kBq}/20 \mu\text{g}/\text{mouse}$ ,  $2.03 \text{ TBq}/\text{mmol}$  ( $54.83 \text{ mCi}/\text{mmol}$ )]. A dramatic decrease in blood pool activity was observed up to 4 days p.i. ( $2.63 \pm 0.93\% \text{ ID/g}$  at 1 day vs  $0.26 \pm 0.11\% \text{ ID/g}$  at 4 days). Maximum tumor accumulation was observed at 1 day p.i., with  $\sim 68\%$  of the radioactivity still present in the tumor at 2 days p.i. ( $9.42 \pm 3.75\% \text{ ID/g}$  vs  $6.44 \pm 3.07\% \text{ ID/g}$ ). While tumor uptake further decreased at 4 days p.i., tumor-to-background ratios increased from 1 to 2 days p.i. ( $3.58$  vs  $5.11$ ), showing only a slight decrease at 4 days p.i. ( $4.69$ ). In all cases, low bone uptake was observed over time, which demonstrates the stability of the  $^{95}\text{Nb}$ -Df complex.

Tumor uptake of  $^{95}\text{Nb}$ -Df-bevacizumab was lower than that observed with bevacizumab labeled with other isotopes (Chang et al., 2013; Nagengast et al., 2007; Nayak et al., 2011; Stollman et al., 2008) and this may be due to the differences in the available target for the antibody. While bevacizumab has high binding affinity to all VEGF-A isoforms, the M165 cell line used in our experiments overexpresses the VEGF-165 isoform, which is partly cell- and ECM-associated and partly secreted from the cells. This could be the reason for the observed washout from the tumor. Another point to be considered is that the specific activity of our radiolabeled product ( $2.03$

TBq/mmol or 54.83 mCi/mmol) was lower than for other groups, with specific activities ranging from 50 MBq/mg (7.50 TBq/mmol or 202.57 mCi/mmol) (Nagengast et al., 2007) to 1.5 GBq/mg antibody (224.89 TBq/mmol or 6.07 Ci/mmol) (Nayak et al., 2011). Finally, the use of 20µg of <sup>95</sup>Nb-Df-bevacizumab per mouse for biodistribution studies may have resulted in accelerated and increased clearance of the radiotracer in the absence of IgG production by nude mice (Sharkey et al., 1991). Nonetheless, the tumor-to-blood ratios of our experiments are higher than those that have been shown by other groups.

The preinjection of an excess of unlabeled bevacizumab prior to <sup>95</sup>Nb-Df-Bevacizumab resulted in a significant reduction in tumor uptake ( $1.22 \pm 0.38$  %ID/g vs  $0.68 \pm 0.02$  %ID/g,  $p < 0.037$ ), leading to the conclusion that <sup>95</sup>Nb-Df-bevacizumab binds specifically to VEGF *in vivo*. A slight increase in radiotracer uptake in the normal tissues was also observed, which is probably attributable to the fact that unlabeled bevacizumab blocks the available VEGF binding sites in tumors, thus leading to an excess of <sup>95</sup>Nb-Df-bevacizumab in the circulation. This is also demonstrated in <sup>95</sup>Nb-Df-bevacizumab blood levels of mice injected pretreated with excess antibody, which are significantly higher than in those without excess antibody ( $0.64 \pm 0.24$  %ID/g vs  $0.26 \pm 0.12$  %ID/g, respectively,  $p < 0.05$ ) (Nayak et al., 2011; Collingridge et al., 2002).

## 5. Conclusions

Obtained data clearly showed excellent labeling, and excellent stability of <sup>95</sup>Nb-Df- bevacizumab *in vitro* and *in vivo*. The <sup>95</sup>Nb/Zr separation chemistry developed should allow the synthesis of <sup>90</sup>Nb-Df-bevacizumab following the <sup>90</sup>Zr (p,n) production process at high specific activity of >100 Mbq/mg mab. This PET tracer will be used to reproduce the promising results shown here with <sup>95</sup>Nb-Df-bevacizumab and further validate its potential for application in *immuno*-PET. In conclusion, we believe that <sup>90</sup>Nb-Df-bevacizumab would be a valuable tool not only for the



selection of patients most likely to benefit from antiangiogenic therapies targeting VEGF-A, but also for the selection of appropriate candidates to undergo  $^{95}\text{Nb}$ -RIT.

## **Acknowledgments**

The authors gratefully acknowledge financial support from the COST Actions TD1004 (Theranostics Imaging and Therapy: An Action to Develop Novel Nanosized Systems for Imaging-Guided Drug Delivery) and D38 (Metal-Based Systems for Molecular Imaging Applications), the Programme for the Promotion of the Exchange and Scientific Cooperation between Greece and Germany IKYDA 2013 (Contract No. 205), the People Programme (Marie Curie Actions) of the European Union's seventh Framework Programme (FP7/2007-2013) under REA grant agreement no.PITN-GA-2012-317019 'Trace'n Treat', and the Deutsche Forschungsgemeinschaft (DFG) under grant DFG Ro 985/40 – 1. Acknowledgements are also due to Mr. Stavros Xanthopoulos, for technical assistance. We also acknowledge the teams of BR2, ILL and TRIGA Mainz.

## References

1. Busse, S., Rösch, F., Qaim, S.M., 2002a. Cross section data for the production of the positron emitting niobium isotope  $^{90}\text{Nb}$  via the  $^{90}\text{Zr}$  ( $p, n$ )-reaction. *Radiochim. Acta.* 90, 1.
2. Busse, S., Brockmann, J., Roesch, F., 2002b. Radiochemical separation of no-carrier-added radioniobium from zirconium targets for application of  $^{90}\text{Nb}$ -labelled compounds. *Radiochim. Acta.* 90, 411-415.
3. Chang, A.J., et al., 2013. Detection of rapalog-mediated therapeutic response in renal cancer xenografts using  $^{64}\text{Cu}$ -bevacizumab immunoPET. *PLoS ONE.* 8 (3), e58949
4. Chacko, A.M., et al., 2014. Development of  $^{124}\text{I}$  immuno-PET targeting tumor vascular TEM1/endsialin. *J. Nucl. Med.* 55 (3), 500-507.
5. Collingridge, D.R., et al., 2002. The development of [ $^{124}\text{I}$ ]Iodinated-VG76e: A novel tracer for imaging vascular endothelial growth factor in vivo using positron emission tomography. *Cancer. Res.* 62 (20), 5912-5919.
6. Ferrara, N., Hillan, K.J., Novotny, W., 2005. Bevacizumab (Avastin), a humanized anti-VEGF monoclonal antibody for cancer therapy. *Biochem. Biophys. Res. Commun.* 333 (2), 328–335.
7. Nagengast, W.B., et al., 2007. In vivo VEGF imaging with radiolabeled bevacizumab in a human ovarian tumor xenograft. *J. Nucl. Med.* 48 (8), 1313–1319.

8. Nagengast, W.B, et al., 2010.  $^{89}\text{Zr}$ -bevacizumab PET of early antiangiogenic tumor response to treatment with HSP90 inhibitor NVP-AUY922. *J. Nucl. Med.* 51, 761–767.
9. Nayak, T.K., Brechbiel, M.W., 2011.  $^{86}\text{Y}$  based PET radiopharmaceuticals: radiochemistry and biological applications. *Med. Chem.* 7 (5), 380-388.
10. Nayak, T.K., 2011. PET imaging of tumor angiogenesis in mice with Vegf-A-targeted  $^{86}\text{Y}$ -chx-a"-dtpa-bevacizumab. *Int. J. Cancer.* 128 (4), 920–926.
11. Radchenko, V., et al., 2012.  $^{90}\text{Nb}$  – a Potential PET Nuclide: production and labeling of monoclonal antibodies. *Radiochim. Acta.* 100 (11),
12. Radchenko, V., et al., 2016. Labeling and preliminary *in vivo* assessment of Niobium-labeled radioactive species: a proof-of-concept study. *Nucl. Med. Biol (accepted)*.
13. Radchenko, V., Busse, S., Roesch, F., 2014. Desferrioxamine as an appropriate chelator for  $^{90}\text{Nb}$ : Comparison of its complexation properties for M-Df-Octreotide (M=Nb, Fe, Ga, Zr). *Nucl. Med. Biol.* 41 (9), 721–727.
14. Severin, G.W., et al., 2011.  $^{89}\text{Zr}$  radiochemistry for positron emission tomography. *Med. Chem.* 7 (5), 389-394.
15. Sharkey, R.M., et al., 1991. Rapid blood clearance of immunoglobulin G2a and immunoglobulin G2b in nude mice. *Cancer. Res.* 51 (12), 3102-3107.
16. Stollman, T.H., et al., 2008. Specific imaging of VEGF-A expression with radiolabeled anti-VEGF monoclonal antibody. *Int. J. Cancer.* 122 (10), 2310–2314.
17. Stollman, T.H., et al., 2009. Tumor accumulation of radiolabeled bevacizumab due to targeting of cell- and matrix-associated VEGF-A isoforms. *Cancer. Biother. Radiopharm.* 24 (2), 195-200.
18. Tolmachev, V., 2011. Radiobromine-labelled tracers for positron emission tomography: possibilities and pitfalls. *Curr. Radiopharm.* 4 (2), 76-89.
19. Van Dongen, G.A., et al., 2007. Immuno-PET: A Navigator in Monoclonal Antibody Development and Applications. *Oncologist.* 12 (12), 1379–1389.

20. Verel, I., et al., 2003.  $^{89}\text{Zr}$  Immuno-PET: Comprehensive procedures for the production of  $^{89}\text{Zr}$ -labeled monoclonal antibodies. *J. Nucl. Med.* 44 (8), 1271–1281.
21. Vosjan, M.J., et al., 2010. Conjugation and radiolabeling of monoclonal antibodies with zirconium-89 for PET imaging using the bifunctional chelate p-isothiocyanatobenzyl-desferrioxamine. *Nat. Protocols.* 5 (4), 739–743.
22. Vugts, D.J., Visser, G.W., van Dongen, G.A., 2013.  $^{89}\text{Zr}$ -PET radiochemistry in the development and application of therapeutic monoclonal antibodies and other biologicals. *Curr. Top. Med. Chem.* 13 (4), 446-457.

## Figure Legends

**Table 1.** Main characteristics of the most commonly-used PET nuclides (Van Dongen et al., 2007).

**Figure 1:** Immunoreactivities of radiolabelled Bevacizumab;  $^{99\text{m}}\text{Tc}$ -bevacizumab (partial reduction of disulfide bonds of antibody),  $^{95}\text{Nb}$ - Df-Bevacizumab. Immunoreactivity of the antibody was calculated as bound counts x 100/total counts

**Figure 2:** Cell binding studies on M165 cells incubated with increasing concentrations of  $^{95}\text{Nb}$ - Df-bevacizumab.

**Figure 3.** Biodistribution of  $^{95}\text{Nb}$ -Df-bevacizumab (270 kBq/20  $\mu\text{g}$ /mouse, [2.03 TBq/mmol (54.83 mCi/mmol)] in tumor-bearing mice

**Table 2.** Tumor-to-blood ratios of injected  $^{95}\text{Nb}$ -Df-bevacizumab

Table 1

Positron emitter	Half-life (hours)	Main $\beta^+$ energies	
		(keV)	(%)
$^{68}\text{Ga}$	1,13	1,899	87,9
$^{18}\text{F}$	1,83	634	100,0
$^{64}\text{Cu}$	12,7	653	17,4
$^{86}\text{Y}$	14,7	1,221	11,9
		1,545	5,6
$^{76}\text{Br}$	16,2	871	6,3
		990	5,2
		3,382	25,8
		3,941	6,0
$^{89}\text{Zr}$	78,4	897	22,7
$^{124}\text{I}$	100,3	1,535	11,8
		2,138	10,9

Figure 1

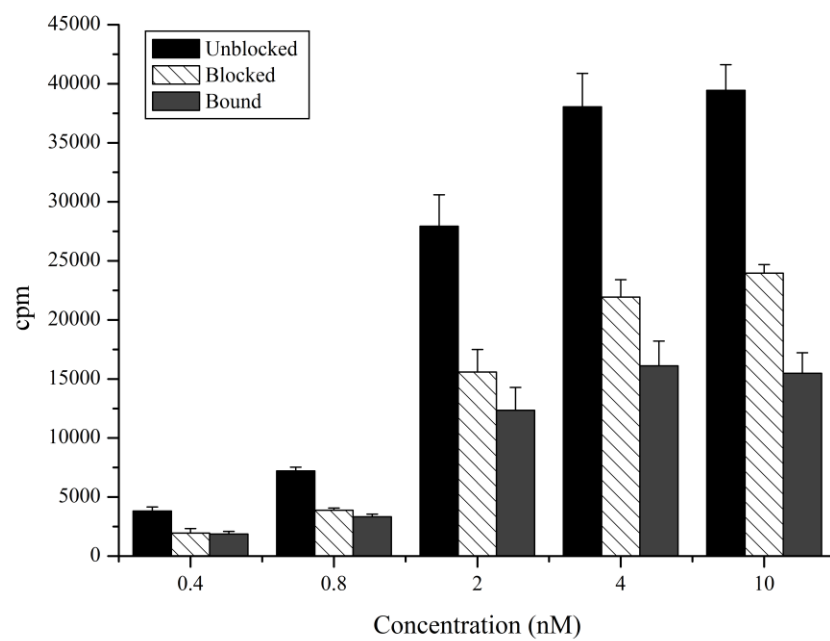


Figure 2

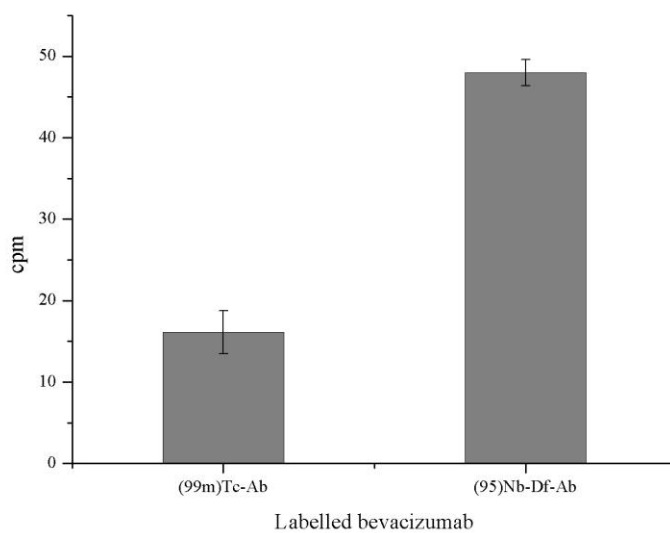


Figure 3

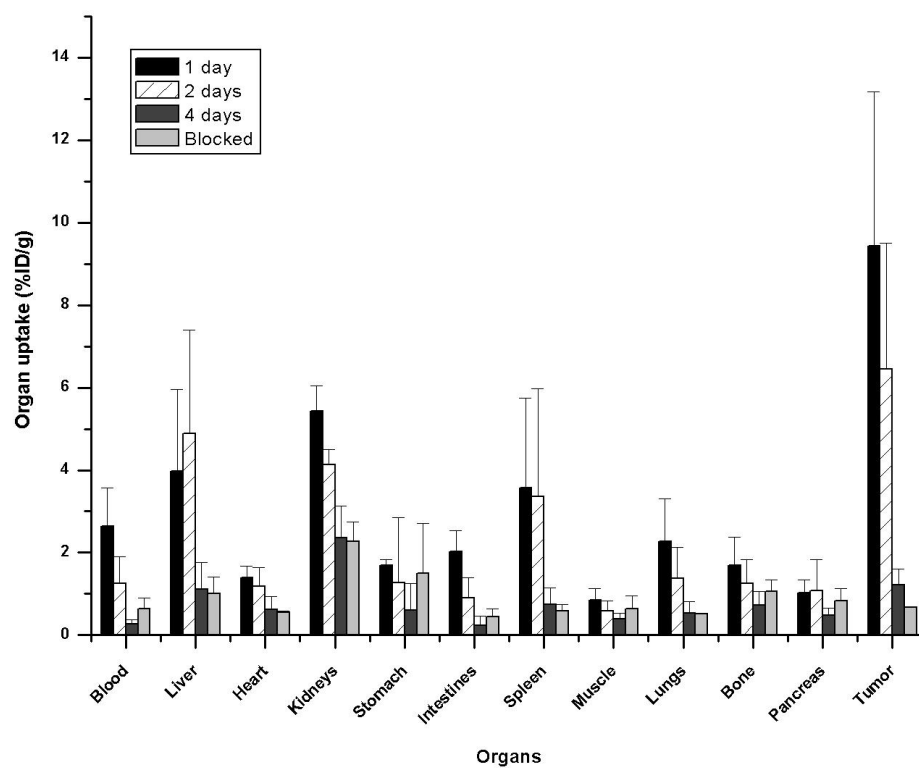


Table 2

1 day	2 days	4 days	4-day blocking
3.58	5.11	4.69	1.06